HHS Public Access

Author manuscript

Mol Cancer Ther. Author manuscript; available in PMC 2016 September 01.

Published in final edited form as:

Mol Cancer Ther. 2015 September ; 14(9): 2014–2022. doi:10.1158/1535-7163.MCT-15-0116.

Small molecule inhibition of MERTK is efficacious in non-small cell lung cancer models independent of driver oncogene status

Christopher T. Cummings[1,*], **Weihe Zhang**[2,5,*], **Kurtis D. Davies**[1], **Gregory D. Kirkpatrick**[1], **Dehui Zhang**[2], **Deborah DeRyckere**[1], **Xiaodong Wang**[2], **Stephen V. Frye**[2,3], **H. Shelton Earp**[3,4], and **Douglas K. Graham**[1,6]

[1]Department of Pediatrics, Section of Hematology, Oncology, and Bone Marrow Transplantation, University of Colorado Anschutz Medical Campus, Aurora, CO 80045 USA

[2]Center for Integrative Chemical Biology and Drug Discovery and Division of Chemical Biology and Medicinal Chemistry, Eshelman School of Pharmacy, University of North Carolina at Chapel Hill, Chapel Hill, NC 27599, USA

[3]Department of Medicine, UNC Lineberger Comprehensive Cancer Center, Chapel Hill, NC 27599, USA

[4]Department of Pharmacology, School of Medicine, University of North Carolina at Chapel Hill, Chapel Hill, NC 27599, USA

Abstract

Treatment of non-small cell lung cancer (NSCLC) has been transformed by targeted therapies directed against molecular aberrations specifically activated within an individual patient's tumor. However, such therapies are currently only available against a small number of such aberrations, and new targets and therapeutics are needed. Our laboratory has previously identified the MERTK receptor tyrosine kinase (RTK) as a potential drug target in multiple cancer types, including NSCLC. We have recently developed UNC2025 – the first-in-class small molecule inhibitor targeting MERTK with pharmacokinetic properties sufficient for clinical translation. Here we utilize this compound to further validate the important emerging biologic functions of MERTK in lung cancer pathogenesis, to establish that MERTK can be effectively targeted by a clinically translatable agent, and to demonstrate that inhibition of MERTK is a valid treatment strategy in a wide variety of non-small cell lung cancer cell lines independent of their driver oncogene status, including in lines with an *EGFR* mutation, a *KRAS/NRAS* mutation, an RTK fusion, or another or unknown driver oncogene. Biochemically, we report the selectivity of UNC2025 for MERTK, and its inhibition of oncogenic downstream signaling. Functionally, we demonstrate that UNC2025 induces apoptosis of MERTK-dependent NSCLC cell lines, while decreasing colony formation *in vitro* and tumor xenograft growth *in vivo* in murine models. These findings provide further

[6]Corresponding Author: Douglas K. Graham, MD, PhD; Department of Pediatrics, Section of Hematology, Oncology and Bone Marrow Transplantation, University of Colorado Anschutz Medical Campus, Mail Stop 8302, 12800 East 19th Avenue, P18-4400, Aurora, CO 80045, USA; doug.graham@ucdenver.edu; Phone: (303) 724-4006; Fax: (303) 724-4015.

[5]Current address: BioCryst Pharmaceuticals, Inc., 2190 Parkway Lake Drive, Birmingham, AL 35244

[*]These authors contributed equally to this work.

Conflicts of Interest: DKG, SVF, HSE, XW, and DD are stockholders in Meryx, Inc. XW, WZ, and SVF have filed a patent describing UNC2025 (intellectual property rights).

evidence for the importance of MERTK in NSCLC, and demonstrate that MERTK inhibition by UNC2025 is a feasible, clinically relevant treatment strategy in a wide variety of NSCLC subtypes, which warrants further investigation in clinical trials.

Keywords

MERTK; Non-Small Cell Lung Cancer; Small Molecule Inhibitor; Targeted Therapy; Receptor Tyrosine Kinase

Introduction

Personalized medicine – therapy against the activated molecular targets within an individual patient's tumor – has transformed the field of clinical oncology. However, few personalized therapeutics are currently available, and the majority of cancer patients still receive conventional cytotoxic regimens. In NSCLC, for example, targeted therapies against activated EGFR or ALK improve survival compared to conventional chemotherapy, but only approximately 10% of newly diagnosed patients have a tumor with an activating *EGFR* mutation, while just 5% have an *ALK* translocation (1–5). For the remaining 85% of patients, opportunities clearly exist to identify new therapeutic targets and compounds.

Our laboratory and others have investigated the role of the TAM family, consisting of the RTK's TYRO3, AXL, and MERTK, in NSCLC. AXL has been well established as a promising target in primary and therapy-resistant NSCLC (6,7). AXL expression is detected in 48% – 93% of patient samples, correlates with an invasive phenotype in cell lines, and with lymph node status and clinical stage in patients (8,9). Additionally, AXL has been shown to mediate resistance to conventional cytotoxic chemotherapeutics, as well as to EGFR-targeted agents (8, 10, 11). MERTK is also over-expressed or ectopically expressed in a multitude of human cancers, and activates a diverse network of downstream pro-oncogenic signaling pathways (8, 12–20). In NSCLC, MERTK is over-expressed in approximately two-thirds of patient tumor samples, regardless of histology (8). Additionally, activation of MERTK in NSCLC cell lines induces pro-oncogenic signaling, and genetic inhibition of MERTK using shRNA decreases this signaling, resulting in increased apoptosis, increased chemosensitivity, decreased colony formation *in vitro*, and inhibition of tumor formation in a murine subcutaneous xenograft model (8). Finally, a monoclonal antibody against MERTK decreases colony formation and increases chemosensitivity to carboplatin, further validating the multiple functional roles of MERTK in NSCLC (21).

As our laboratory and others have validated MERTK as a promising target in NSCLC and other cancers, we have taken the next step of developing therapies against MERTK, including a monoclonal antibody (21, 22), and small molecule TKIs (17, 23–27). We have previously published on the synthesis and structure-activity relationships of several first-generation tool compound TKIs, and here report the pre-clinical characterization of UNC2025, the first with sufficient pharmacokinetic properties for murine-based studies and potential clinical translation (28). UNC2025 is approximately 15-fold selective for MERTK over AXL, and MERTK is the most potently inhibited kinase, with the exception of FLT3. UNC2025 is approximately equipotent against FLT3 and MERTK. While known to play

important roles in subsets of acute myeloid leukemia, where it is constitutively activated through mutation, FLT3 has not been shown to be expressed in NSCLC, and therefore effects of UNC2025 in NSCLC are likely to be MERTK-dependent (29). In addition, UNC2025 is approximately 20-fold selective for MERTK over TYRO3, and has more than 700-fold selectivity for MERTK over MET, another closely related RTK to the TAM family with established roles in NSCLC. In this study, we demonstrate selectivity of UNC2025 for MERTK within the TAM family in NSCLC cells, UNC2025-mediated abrogation of MERTK-mediated pro-oncogenic downstream signaling, and functional consequences, including induction of cellular apoptosis and decreased colony formation *in vitro*, and inhibition of tumor growth *in vivo*. Additionally, we demonstrate that UNC2025 is broadly efficacious in a wide variety of cell lines, independent of driver oncogene status. Specifically, UNC2025 retained potent efficacy against cell lines containing an *EGFR* mutation, a *KRAS/NRAS* mutation, an RTK fusion, or another or unknown driver oncogene. These results support further consideration of testing UNC2025 in clinical trials.

Materials and Methods

Cell culture and treatment

All cell lines were maintained in RPMI medium supplemented with 10% fetal bovine serum (FBS), penicillin (100 U/mL), and streptomycin (100 μg/ml) until plating for experiments. Specific culture conditions for each experiment are provided within the relevant sub-sections below. All cell line identities were confirmed by the authors by comparison of short tandem repeat profiles to publically available databases. Testing was performed at the time of acquisition of each cell line, as well as approximately annually thereafter. Validated STR profiles were not available for some of the cell lines (H157, H3122, HCC4011, SF188) but the profiles obtained did not match any other cell line. The A172, A549, G361, H226, H1299, H2009, HMCB, and U251 cell lines were purchased from the American Type Culture Collection (ATCC, Manassas, VA), the Colo699 cell line was purchased from the German Collection of Microorganisms and Cell Cultures (DSMZ, Braunschweig, Germany), the SF188 cell line was obtained from the UCSF Brain Tumor Bank, and the Calu3, H157, H322, H358, H441, H460, H1650, H1975, H2126, H2228, H3122, H3255, HCC827, HCC4006, HCC4011, and LC-2/ad cell lines were obtained from Drs. John Minna and Adi Gazdar (University of Texas Southwestern Medical Center, Dallax, TX). UNC2025 and UNC1653 were synthesized as previously described (25, 27).

Western blotting

Cells were either lifted with 0.02% EDTA in PBS and re-suspended in lysis buffer (50 mM HEPES pH 7.5, 150 mM NaCl, 10 mM EDTA, 10% glycerol, 1% Triton X-100, 1 mM Na_3VO_4) supplemented with protease inhibitors (Complete Mini, Roche Molecular Biochemicals) or washed with PBS and scraped into lysis buffer. Total protein concentrations were determined and western blotting was performed as previously described (8).

Antibodies for western blotting

For western blotting, the following antibodies were obtained from Cell Signaling: pAKT (S473, Cat# 9271), AKT (Cat# 9272), pERK1/2 (T202/Y204, Cat# 9106), ERK1/2 (Cat# 9102), c-KIT(Cat# 3074), Survivin (Cat# 2808), α-tubulin (Cat# 2125), and TYRO3 (Cat# 5585). Additional antibodies used for western blotting include AXL (R&D Systems, AF154), FLT3 (Santa Cruz, sc-480), pMERTK (Y749, Y753, Y754, PhosphoSolutions), MERTK (Abcam ab52968), pan-TRK (Santa Cruz, sc-11), and pTyrosine (4G10 Platinum, Millipore 05-1050). Horseradish peroxidase (HRP)-conjugated secondary antibodies (goat anti-rabbit, Bio-Rad 170-6515; goat anti-mouse, Bio-Rad 170-6516; donkey anti-goat, Santa Cruz sc-2020) were used for detection of proteins using enhanced chemiluminescence.

Immunoprecipitation and detection of phosphorylated MERTK, AXL, and TYRO3

After one hour of treatment with DMSO, UNC2025, or UNC1653 in RPMI medium supplemented with 10% FBS, penicillin (100 U/mL), and streptomycin (100 μg/ml), cells were treated with pervanadate phosphatase inhibitor (0.12 mM Na_3VO_4 in 0.002% H_2O_2 in PBS) for 5 minutes (A549, H1299, H2228) or 1 minute (Colo699), and then lysed. Lysates were incubated with antibodies against MERTK (R&D Systems, MAB8912), AXL (R&D Systems, AF154), or TYRO3 (Cell Signaling, 5585) and with rec-Protein G-sepharose 4B beads (Invitrogen 10-1242) overnight. Beads were then washed twice with lysis buffer, resuspended in Laemmli buffer (62.5 mM Tris-HCl pH 6.8, 25% glycerol, 5% beta-mercaptoethanol, 2% SDS, and 0.01% bromophenol blue), boiled, and resolved on polyacrylamide gels. Blots were probed for phospho-MERTK or phospho-tyrosine, stripped, and re-probed for total MERTK (Abcam, 52968), AXL (R&D Systems, AF154), or TYRO3 (Cell Signaling, 5585).

Assessment of downstream signaling

Recombinant human Gas6 (rhGas6, 885-GS) was purchased from R&D Systems. Sub-confluent cultures were starved in serum-free medium for two hours and then cultured in the presence of UNC2025 or vehicle control for an additional two hours prior to Gas6 stimulation for 10 minutes. Lysates were quantified by Bradford assay and analyzed by western blot. Alternatively, cultures were treated with UNC2025 or vehicle control for 72 hours in RPMI medium supplemented with 10% FBS, penicillin (100 U/mL), and streptomycin (100 μg/ml), prior to lysis, quantification, and analysis on western blot (Supplemental Figure 2).

Assessment of apoptosis and cell death

A549, Colo699, H1299, and H2228 cells were treated with UNC2025, UNC1653, or DMSO vehicle control for 72 hours in RPMI medium supplemented with 10% FBS, penicillin (100 U/mL), and streptomycin (100 μg/ml). Supernatants were collected and combined with cells after lifting with EDTA. Cells were then stained with 0.2 μM YO-PRO®-1-iodide (YO-PRO-1) and 1.5 μM propidium iodide (PI) (Invitrogen). Uptake of dyes was assessed by flow cytometry using an FC500 cytometer and CXP analysis software (Beckman Coulter).

Soft agar colony formation assay

15,000 cells per well were plated in 0.35% Noble agar in RPMI, and overlaid on 0.5% Noble agar in RPMI in 6-well plates. Agar layers were overlaid with 2 mL RPMI medium supplemented with 10% FBS, penicillin (100 U/mL), and streptomycin (100 μg/ml) containing DMSO vehicle control, UNC2025, or UNC1653. This medium layer was aspirated and replaced three times per week. After two weeks of growth, medium was aspirated, and cells were stained with 200 uL nitrotetrazoline blue chloride (NTB) (Biosynth N-8100) overnight. Colonies were then counted using a GelCount colony counter and software (Oxford Optronix).

Subcutaneous xenograft model

All experiments involving animals were approved by the University of Colorado Institutional Animal Care and Use Committee. Two million H2228 cells or 5.5 million A549 cells were suspended in 100 uL PBS (with 50% Matrigel for the A549 cell line) and injected subcutaneously into the flank of athymic Nude-*Foxn1*^{nu} mice. Tumors were measured weekly with calipers, and volume was calculated using the formula Volume=$\pi a^2 b/6$, where 'a' represents the shortest diameter measured perpendicular to the longest diameter, 'b'. When tumors reached an average size of 100-200 mm^3, mice were randomized to groups and treated twice daily by oral gavage with saline or UNC2025 at 30 mg/kg or 50 mg/kg, administered at a dose of 10 ml/kg.

Statistical analysis

Statistical analyses were performed using Prism 5 software (GraphPad Software, Inc.). An unpaired t-test was used for analysis of apoptosis and xenograft assays, a paired t-test was used for analysis of soft agar colony number after normalization to vehicle-treated controls wihin each replicate, and IC_{50} values were calculated using Segmental Linear Regression. All data are representative of at least three independent experiments.

Results

UNC2025 Selectively Inhibits MERTK Phosphorylation

To test the selectivity of UNC2025 within the TAM family, levels of phosphorylated MERTK, AXL, and TYRO3 were assessed in H2228, A549, Colo699, and H1299 cells after one hour of treatment with UNC2025 or UNC1653, a negative control compound that lacks activity against MERTK (27) (Figure 1A). UNC2025 potently inhibited MERTK phosphorylation at doses in the low nanomolar range, with IC_{50} values below 50 nM in all four cell lines studied (Figure 1B). In addition, UNC2025 was selective for MERTK over the related kinases AXL and TYRO3. Phospho-AXL was expressed in the H2228, A549, and H1299 cell lines, while Colo699 cells did not express AXL. Phospho-TYRO3 was expressed in the H2228, H1299, and A549 cell lines, but was not reliably detected in the Colo699 cell line. Regardless of expression levels, treatment with UNC2025 at doses up to 300 nM was far less potent against phospho-AXL or phospho-TYRO3 than against phospho-MERTK in any of these cell lines. Importantly, AXL and TYRO3 were two of the most potently inhibited kinases after MERTK in enzymatic assays characterizing the

specificity of UNC2025 against a panel of over 300 kinases (28). Other kinases determined to have greater sensitivity to UNC2025 than AXL and TYRO by this *in vitro* screening assay include FLT3, c-KIT, and TRKA, however, none of these proteins were expressed in any of the four cell lines studied (Supplemental Figure 1). All other of the 300+ kinases assayed in the selectivity profiling are predicted to be less sensitive to UNC2025 than even TYRO3, and thus MERTK appears to be the only relevant target inhibited by UNC2025 in these cell lines and at these concentrations. While it is impossible to rule out the contribution of partial inhibition of other kinases to the effects observed with UNC2025, our extensive characterization of the translation of *in vitro* potency to cellular phospho-protein potency demonstrates that kinases less inhibited by UNC2025 than TYRO3 *in vitro* would also be expected to be less inhibited in cells, and therefore less than 50% inhibited at doses up to 300 nM (25). Finally, UNC1653 did not decrease phosphorylation of MERTK at doses up to 300 nM (Figure 1C). Interestingly, total MERTK expression was increased in response to treatment with higher doses of UNC2025 in 3 of the 4 lines tested.

Oncogenic Signaling Downstream of MERTK is Blocked by UNC2025

MERTK is known to stimulate a large network of downstream signaling proteins, most commonly through the MAPK and PI3K/AKT pathways (20). To determine whether treatment with UNC2025 abrogated these effects, cells were treated with UNC2025 or vehicle control prior to stimulation with the TAM-family ligand GAS6 (Figure 2A). Decreased levels of pAKT and/or pERK1/2 were detected after UNC2025 treatment in all four cell lines studied; however, effects were cell line specific. In the H2228 cell line, UNC2025 reduced basal levels of both pAKT and pERK1/2 (lane 1 vs. lane 3). Similarly, basal pAKT levels were reduced in the A549 cell line (lane 1 vs. lane 3), while pERK1/2 levels were unaffected. In the Colo699 cell line, pAKT levels were unaffected, however, Gas6-induced pERK1/2 stimulation was inhibited by UNC2025 (lane 2 vs. lane 4). Basal pERK1/2 levels were undetectable in this cell line. Finally, in the H1299 cell line, both basal (lane 1 vs. lane 3) and stimulated (lane 2 vs. lane 4) pAKT and pERK1/2 were decreased by UNC2025 administration.

Unexpectedly, and in contrast to the Colo699 and H1299 cell lines, GAS6 induced a decrease of pAKT and pERK1/2 in the H2228 and A549 cell lines at the one hour time-point measured. Compensatory regulatory mechanisms are hypothesized to play a role in this effect, as has been shown to be the case in other oncogenic signaling pathways, however specific negative regulatory pathways here remain unidentified (30). In spite of these paradoxical effects of GAS6, positive effects of UNC2025 were demonstrated in all four cell lines assayed. However; long-term signaling assays were next utilized in order to identify a more conserved downstream marker of UNC2025 response. Cultures were treated with 300 nM UNC2025 for 72 hours, lysed, and analyzed by western blot. Survivin, a member of the inhibitor of apoptosis protein (IAP) family, was consistently decreased after UNC2025 treatment (Figure 2B). As Survivin has been shown to be a promising drug target, we sought to determine whether Survivin levels were decreased in response to UNC2025 treatment in additional solid tumor cell lines representing a variety of tumor types (31). We treated four additional NSCLC cell lines, three glioblastoma cell lines, and two melanoma cell lines with UNC2025, and examined Survivin levels in whole cell lysates. In 10 of the 13 solid tumor

cell lines assessed, Survivin levels were dramatically decreased. Survivin protein expression was decreased in six of the eight total NSCLC cell lines assessed, all three glioblastoma cell lines, and one of the two melanoma cell lines (Supplemental Figure 2).

pAKT, pERK1/2, and Survivin are all well-validated targets in the mechanism of action of NSCLC pathogenesis, and indeed all three have therapeutics in various stages of clinical trials for lung cancer patients (32, 33). The inhibition of these targets by UNC2025 suggested mechanisms of action by which functional effects would be expected to occur, and that such functional testing was warranted.

MERTK Inhibition by UNC2025 Induces Apoptotic Cell Death

We next hypothesized that the potent effects mediated by UNC2025 on MERTK phosphorylation and downstream oncogenic signaling would translate to a functional decrease in survival of NSCLC cells. To test this hypothesis, NSCLC cells were treated with 300 nM UNC2025 or UNC1653 for 72 hours, stained with YO-PRO-1 and PI dyes, and analyzed by flow cytometry to assess apoptotic cell death. Treatment with UNC2025, but not UNC1653, significantly increased the fraction of apoptotic and dead cells in all four cell lines studied (Figure 3). UNC2025 increased cell death from basal levels of 23.9±4.2%, 13.8±2.2%, 9.9±1.6%, and 44.2±0.1%, in the H2228, A549, Colo699, and H1299 cell lines, to 40.5±3.8%, 50.3±7.1%, 32.9±6.2%, and 59.1±3.4%, respectively ($p = 0.0428$, $p=0.0081$, $p=0.0224$, $p=0.0118$). Levels of apoptosis were not significantly different from basal levels after UNC1653 treatment in any of the four NSCLC cell lines.

UNC2025 Decreases Colony-Formation in a Dose-Dependent Manner

A soft agar assay was utilized to determine the long-term functional effects of UNC2025 treatment on NSCLC colony formation. UNC2025, UNC1653, or vehicle control was administered three times per week. After two weeks of growth, colonies were stained and counted (Figure 4A). Treatment with UNC2025, but not UNC1653, significantly reduced colony formation of all four NSCLC cell lines assayed (Figure 4B). At a dose of 300nM UNC2025, colony formation was reduced by 99.2%, 98.1%, 98.2%, and 80.1%, in the H2228, A549, Colo699, and H1299 cell lines, respectively ($p<0.0001$ for each).

Since UNC2025 robustly decreased colony formation in all four of the studied NSCLC cell lines, we sought to determine if this trend was conserved in a larger panel of NSCLC cell lines with different driver oncogene statuses. Cell lines harboring an *EGFR* mutation, an RTK fusion, a *KRAS* or *NRAS* mutation, and those with another or with no known driver were assessed in the soft agar assay. IC_{50} values were calculated for each cell line (Figure 4C). Driver oncogene status did not correlate with sensitivity to UNC2025, as IC_{50}'s between 50nM and 350 nM were observed in cell lines of each type studied. Similarly, expression of MERTK or phospho-MERTK also did not correlate with sensitivity to UNC2025. As seen in Supplemental Figure 3, cell lines were arranged from most to least sensitive, utilizing the IC_{50} values from Figure 4C, and assayed for pMERTK levels by immunoprecipitation, or total MERTK levels by western blot of whole cell lysates. Although all cell lines express pMERTK/MERTK, levels of both variably increase and decrease from the most sensitive to least sensitive cell lines, indicating a lack of predictive

value for response. This is potentially due to the activation of alternative signaling pathways present in these cell lines, however, these remain unidentified at this time.

UNC2025 Inhibits Tumor Growth in Murine Models

As UNC2025 shows potent anti-tumor effects *in vitro*, and since it has the pharmacokinetic properties for *in vivo* administration, we determined the effects of UNC2025 *in vivo* in murine subcutaneous xenograft models. Mice were injected with H2228 (Figure 5A) or A549 (Figure 5B) NSCLC cells and tumors were established until an average size of approximately 100 cubic millimeters (A549) or 150 cubic millimeters (H2228) was reached. Mice were then treated twice daily by oral gavage with either saline vehicle or 50 mg/kg UNC2025 and tumor size was measured weekly. Tumor growth was significantly impaired in mice treated with UNC2025, as indicated by significantly smaller tumor volumes relative to mice treated with saline at every measurement point in the H2228 cell line ($p=0.0193$, $p=0.0058$, $p=0.0011$, and $p=0.0034$ after one, two, three, and four weeks of treatment, respectively). In the A549 cell line, tumor volume between the two groups were significantly different during the final two weeks of measurements ($p=0.0021$ and $p=0.0015$, respectively). At the end of the study period in the H2228 study, tumor volume was reduced by 70.2%, from 1183±258 mm^3 in saline-treated mice, to 352±51 mm^3 in mice that had received UNC2025. In the A549 cell line study, final tumor volume was reduced by 61.9%, from 373±57 mm^3 in saline-treated mice, to 143±28 mm^3 in UNC2025-treated mice. Additionally, in a dose-reduction study, mice were again injected with A549 tumor cells, and allowed to establish until an average size of approximately 200 mm^3 was reached (Figure 5C). As before, mice were then randomized and treated with saline, 50 mg/kg UNC2025, or a lower-dose treatment arm of 30 mg/kg UNC2025. Mice were again treated twice daily orally, and tumors measured weekly. Tumor growth was nearly completely inhibited in both treatment arms of this study, and there was no significant difference between the doses of UNC2025. To further analyze the mechanism behind this effect, a pharmacokinetic study assaying concentrations of UNC2025 in the plasma and tumors of mice post-treatment was utilized. Mice harboring established A549 tumors were treated twice daily for three days with saline or UNC2025 at 30 mg/kg or 50 mg/kg, in order to establish a steady-state level. Plasma and tumors were harvested one or 12 hours after the final treatment, to capture peak and trough concentrations of UNC2025. Specimens were analyzed by LC-MS/MS for compound concentration (Supplemental Table 1). Importantly, trough concentrations of 161 nM and 50 nM were found in plasma of mice treated with 50 mg/kg and 30 mg/kg UNC2025, respectively, well within the 50 – 300 nM range utilized within the functional assays in this manuscript. In light of this, it is somewhat unsurprising that these doses are equally efficacious in Figure 5C, as both maintain trough levels above 50 nM; however, 30 mg/kg may be nearing the minimum effective dose, as doses lower than 50 nM are relatively ineffective in *in vitro* assays previously shown.

Discussion

MERTK was initially cloned from a B-lymphoblastoid expression library and its role in a wide variety of blood cancers has subsequently been extensively characterized (7, 34). More recently, it has become increasingly appreciated that MERTK plays important roles in solid

tumors as well. In NSCLC in particular, MERTK is aberrantly expressed in approximately two-thirds of patient tumors, and its activation results in increased downstream pro-oncogenic signaling. Genetic inhibition of MERTK by shRNA in NSCLC cells inhibits this signaling network, resulting in induction of apoptosis, decreased colony formation *in vitro*, enhanced chemosensitivity, and decreased tumor formation *in vivo* in a murine model (8). MERTK was further validated as an important target in NSCLC by the finding that Mer590, a monoclonal antibody targeting MERTK, decreases pro-oncogenic signaling, increases apoptosis, increases chemosensitivity, and decreases colony formation in NSCLC cell lines (21). Importantly, two of the cell lines used in the current study, A549 and Colo699, were used extensively in the shRNA target validation and Mer590 monoclonal antibody studies, respectively. The consistency between the effects observed in these studies using three different mechanisms of MERTK inhibition provides strong support that the observed phenotypes are indeed MERTK-dependent.

MERTK has been extensively validated as a potential therapeutic target not only in NSCLC, but also in a multitude of other cancers. For this reason, our group recently began pursuing the synthesis of novel small molecule tyrosine kinase inhibitors targeting MERTK. We have generated a series of novel compounds representing the first-in-class MERTK-targeted small molecule inhibitors (17, 23–28). UNC2025 is the first compound of these inhibitors with pharmacokinetic properties suitable for *in vivo* study and potential clinical translation. Here, we have investigated the utility of UNC2025 in NSCLC and have demonstrated that UNC2025 is selective for MERTK over related TAM-family members AXL and TYRO3, inhibits downstream signaling through AKT, ERK1/2 and Survivin, induces apoptotic cell death, decreases colony formation *in vitro*, and decreases tumor formation *in vivo* in murine xenograft models. Importantly, sensitivity to UNC2025 did not depend on driver oncogene status. Development of MERTK-selective TKIs for clinical application may therefore provide a molecularly-targeted treatment option for patients without known oncogenic mutations or with a wide variety of alternative driver mutations.

One mechanism by which MERTK inhibition may mediate anti-tumor activity is inhibition of Survivin expression. We have previously demonstrated decreased total levels of Survivin in response to shRNA-mediated MERTK inhibition, and here confirm this finding with UNC2025-mediated MERTK inhibition (8). Survivin plays important roles in several critical aspects of oncogenesis, where it functions to promote tumor cell survival, proliferation, metastasis, and chemoresistance, and can also contribute to tumor angiogenesis (31). Additionally, Survivin is an extremely cancer-specific target, as it is expressed widely in a multitude of cancer types, but not in the vast majority of normal adult tissues. These qualities have made Survivin a top target for new therapy development, and several novel therapies are currently in clinical development. However, early results have not been as impressive as hoped, and additional strategies to target Survivin, including potentially via UNC2025-mediated MERTK inhibition, are needed. Additionally, as MERTK-targeted therapeutics transition to the clinic, pharmacodynamic biomarkers indicating response of the tumor to treatment will become a necessity. Survivin has previously been used as a tumor biomarker due to its tumor-specific expression. We have demonstrated decreased Survivin levels following treatment with UNC2025 in a wide variety of solid tumor cell lines,

including the majority of NSCLC lines assayed. Decreased Survivin expression is a more consistent indicator of UNC2025-mediated MERTK inhibition than changes in phospho-AKT and phospho-ERK levels, and is more easily measured than phospho-MERTK. It is conceivable that Survivin levels could be determined pre- and post-UNC2025 administration as an early marker of tumor response to facilitate clinical decisions regarding therapeutic strategy.

In addition to MERTK, important roles for AXL have also been characterized in NSCLC (6, 8). AXL expression has been correlated with lymph node status and clinical stage in patient tumor samples and can mediate resistance to EGFR-targeted therapy (9–11). Several TKIs against AXL are in various stages clinical development (7). The data presented here suggest that continued development of MERTK-selective TKIs may allow a second TAM-family member to be targeted clinically. Additionally, dual inhibition of both MERTK and AXL represents another potential therapeutic strategy and may be more efficacious than inhibition of either single TAM-family member.

UNC2025 is a novel TKI that is selective for MERTK within the TAM family, inhibits MERTK's downstream signaling network, induces apoptotic cell death and inhibits colony formation in tumor cell cultures independent of driver oncogene status, and decreases tumor growth *in vivo* in murine models. These promising effects mediated by UNC2025 in pre-clinical studies demonstrate that MERTK-targeted TKIs deserve further investigation and optimization toward clinical trials.

Supplementary Material

Refer to Web version on PubMed Central for supplementary material.

Acknowledgments

Financial Support: D.K. Graham is supported by a grant from the NIH (RO1CA137078). K.D. Davies is supported by a grant from the NIH (SPORE in Lung Cancer - P50CA058187), and the Lung Cancer Colorado Fund. This research was funded in part by a research grant from Merck & Co., Inc.

The authors would like to thank Christopher Porter, Karen Helm, Christine Childs, Lester Acosta, Kristina Heide, and Erin Erdahl in the University of Colorado Cancer Center Flow Cytometry Core.

References

1. Maemondo M, Inoue A, Kabayashi K, Sugawara S, Oizumi S, Isobe H, et al. Gefitinib or chemotherapy for non-small-cell lung cancer with mutated EGFR. N Engl J Med. 2010; 362:2380–8. [PubMed: 20573926]
2. Shepherd FA, Rodrigues Pereira J, Cluleanu T, Tan EH, Hirsh V, Thongprasert S, et al. Erlotinib in previously treated non-small-cell lung cancer. N Engl J Med. 2005; 353:123–32. [PubMed: 16014882]
3. Sequist LV, Yang JC, Yamamoto N, O'Byrne K, Hirsh V, Mok T, et al. Phase III study of afatinib or cisplatin plus pemetrexed in patients with metastatic lung adenocarcinoma with EGFR mutations. J Clin Oncol. 2013; 31:3327–34. [PubMed: 23816960]
4. Shaw AT, Kim DW, Nakagawa K, Seto T, Crino L, Ahn MJ, et al. Crizotinib versus chemotherapy in advanced ALK-positive lung cancer. N Engl J Med. 2013; 368:2385–94. [PubMed: 23724913]
5. Minuti G, D'Incecco A, Cappuzzo F. Targeted therapy for NSCLC with driver mutations. Expert Opin Biol Ther. 2013; 13:1402–12.

6. Linger RM, Keating AK, Earp HS, Graham DK. Taking aim at Mer and Axl receptor tyrosine kinases as novel therapeutic targets in solid tumors. Expert Opin Ther Targets. 2010; 14:1073–90. [PubMed: 20809868]
7. Graham DK, DeRyckere D, Davies KD, Earp HS. The TAM family: phosphatidylserine-sensing receptor tyrosine kinases gone awry in cancer. Nat Rev Cancer. 2014; 14:769–85. [PubMed: 25568918]
8. Linger RM, Cohen RA, Cummings CT, Sather S, Migdall-Wilson J, Middleton DH, et al. Mer or Axl receptor tyrosine kinase inhibition promotes apoptosis, blocks growth and enhances chemosensitivity of human non-small cell lung cancer. Oncogene. 2013; 32:3420–31. [PubMed: 22890323]
9. Shieh YS, Lai CY, Kao YR, Shiah SG, Chu YW, Lee HS, et al. Expression of axl in lung adenocarcinoma and correlation with tumor progression. Neoplasia. 2005; 7:1058–64. [PubMed: 16354588]
10. Zhang Z, Lee JC, Lin L, Olivas V, Au V, LaFramboise T, et al. Activation of the AXL kinase causes resistance to EGFR-targeted therapy in lung cancer. Nat Genet. 2012; 44:852–60. [PubMed: 22751098]
11. Brand TM, Iida M, Stein AP, Corrigan KL, Braverman CM, Luthar N, et al. AXL mediates resistance to cetuximab therapy. Cancer Res. 2014; 74:5152–64. [PubMed: 25136066]
12. Linger RM, Lee-Sherick AB, DeRyckere D, Cohen RA, Jacobsen KM, McGranahan A, et al. Mer receptor tyrosine kinase is a therapeutic target in pre-B-cell acute lymphoblastic leukemia. Blood. 2013; 122:1599–609. [PubMed: 23861246]
13. Keating AK, Salzberg DB, Sather S, Liang X, Nickoloff S, Anwar A, et al. Lymphoblastic leukemia/lymphoma in mice overexpressing the Mer (MerTK) receptor tyrosine kinase. Oncogene. 2006; 25:6092–100. [PubMed: 16652142]
14. Brandao LN, Winges A, Christoph S, Sather S, Migdall-Wilson J, Schlegel J, et al. Inhibition of MerTK increases chemosensitivity and decreases oncogenic potential in T-cell acute lymphoblastic leukemia. Blood Cancer J. 2013; 3:e101. [PubMed: 23353780]
15. Graham DK, Salzberg DB, Kurtzberg J, Sather S, Matsushima GK, Keating AK, et al. Ectopic expression of the proto-oncogene Mer in pediatric T-cell acute lymphoblastic leukemia. Clin Cancer Res. 2006; 12:2662–9. [PubMed: 16675557]
16. Lee-Sherick AB, Eisenman KM, Sather S, McGranahan A, Armistead PM, McGary CS, et al. Aberrant Mer receptor tyrosine kinase expression contributes to leukemogenesis in acute myeloid leukemia. Oncogene. 2013; 32:5359–68. [PubMed: 23474756]
17. Schlegel J, Sambade MJ, Sather S, Moschos SJ, Tan AC, Winges A, et al. MERTK receptor tyrosine kinase is a therapeutic target in melanoma. J Clin Invest. 2013; 123:2257–67. [PubMed: 23585477]
18. Keating AK, Kim GK, Jones AE, Donson AM, Ware K, Mulcahy JM, et al. Inhibition of Mer and Axl receptor tyrosine kinases in astrocytoma cells leads to increased apoptosis and improved chemosensitivity. Mol Cancer Ther. 2010; 9:1298–307. [PubMed: 20423999]
19. Wu YM, Robinson DR, Hung HJ. Signal pathways in up-regulation of chemokines by tyrosine kinase MER/NYK in prostate cancer cells. Cancer Res. 2004; 64:7311–20. [PubMed: 15492251]
20. Cummings CT, Deryckere D, Earp HS, Graham DK. Molecular pathways: MERTK signaling in cancer. Clin Cancer Res. 2013; 19:5275–80. [PubMed: 23833304]
21. Cummings CT, Linger RMA, Cohen RA, Sather S, Kirkpatrick GD, Davies KD, et al. Mer590, a novel monoclonal antibody targeting MER receptor tyrosine kinase, decreases colony formation and increases chemosensitivity in non-small cell lung cancer. Oncotarget. 2014; 5:10434–45. [PubMed: 25372020]
22. Rogers AE, Le JP, Sather S, Pernu BM, Graham DK, Pierce AM, et al. Mer receptor tyrosine kinase inhibition impedes glioblastoma multiforme migration and alters cellular morphology. Oncogene. 2012; 31:4171–81. [PubMed: 22179835]
23. Liu J, Yang C, Simpson C, Deryckere D, Van Deusen A, Miley MJ, et al. Discovery of Novel Small Molecule Mer Kinase Inhibitors for the Treatment of Pediatric Acute Lymphoblastic Leukemia. ACS Med Chem Lett. 2012; 3:129–34. [PubMed: 22662287]

24. Liu J, Zhang W, Stashko MA, Deryckere D, Cummings CT, Hunter D, et al. UNC1062, a new and potent Mer inhibitor. Eur J Med Chem. 2013; 65:83–93. [PubMed: 23693152]
25. Zhang W, Zhang D, Stashko MA, Deryckere D, Hunter D, Kireev D, et al. Pseudo-Cyclization through Intramolecular Hydrogen Bond Enables Discovery of Pyridine Substituted Pyrimidines as New Mer Kinase Inhibitors. J Med Chem. 2013; 56:9683–92. [PubMed: 24195762]
26. Christoph S, Deryckere D, Schlegel J, Frazer JK, Batchelor LA, Trakhimets AY, et al. UNC569, a novel small-molecule mer inhibitor with efficacy against acute lymphoblastic leukemia in vitro and in vivo. Mol Cancer Ther. 2013; 12:2367–77. [PubMed: 23997116]
27. Lee-Sherick AB, Zhang W, Menachof KK, Hill AA, Rinella S, Kirkpatrick G, et al. Efficacy of a Mer and Flt3 tyrosine kinase small molecule inhibitor, UNC1666, in acute myeloid leukemia. Oncotarget. in press.
28. Zhang W, DeRyckere D, Hunter D, Liu J, Stashko M, Minson KA, et al. UNC2025, a potent and orally bioavailable MER/FLT3 dual inhibitor. J Med Chem. 2014; 57:7031–41. [PubMed: 25068800]
29. Serve H, Flesch K, Serve S, Fenski R, Berdel WE. Expression and function of Flt3/flk2 in human tumor cell lines. Int J Oncol. 1999; 14:765–70. [PubMed: 10087327]
30. Harris DL, Joyce NC. Protein tyrosine phosphatase, PTP1B, expression and activity in rat corneal endothelial cells. Mol Vis. 2007; 13:785–96. [PubMed: 17563729]
31. Athanasoula, KCh; Gogas, H.; Polonifi, K.; Vaiopoulos, AG.; Polyzos, A.; Mantzourani, M. Survivin beyond physiology: orchestration of multistep carcinogenesis and therapeutic potentials. Cancer Lett. 2014; 347:175–82. [PubMed: 24560928]
32. Reungwetwattana T, Dy GK. Targeted therapies in development for non-small cell lung cancer. J Carcinog. 2013; 12:22. [PubMed: 24574860]
33. Coumar MS, Tsai FY, Kanwar JR, Sarvagalla S, Cheung CH. Treat cancers by targeting survivin: just a dream or future reality? Cancer Treat Rev. 2013; 39:802–11. [PubMed: 23453862]
34. Graham DK, Dawson TL, Mullaney DL, Snodgrass HR, Earp HS. Cloning and mRNA expression analysis of a novel human protooncogene, c-mer. Cell Growth Differ. 1994; 5:647–57. [PubMed: 8086340]

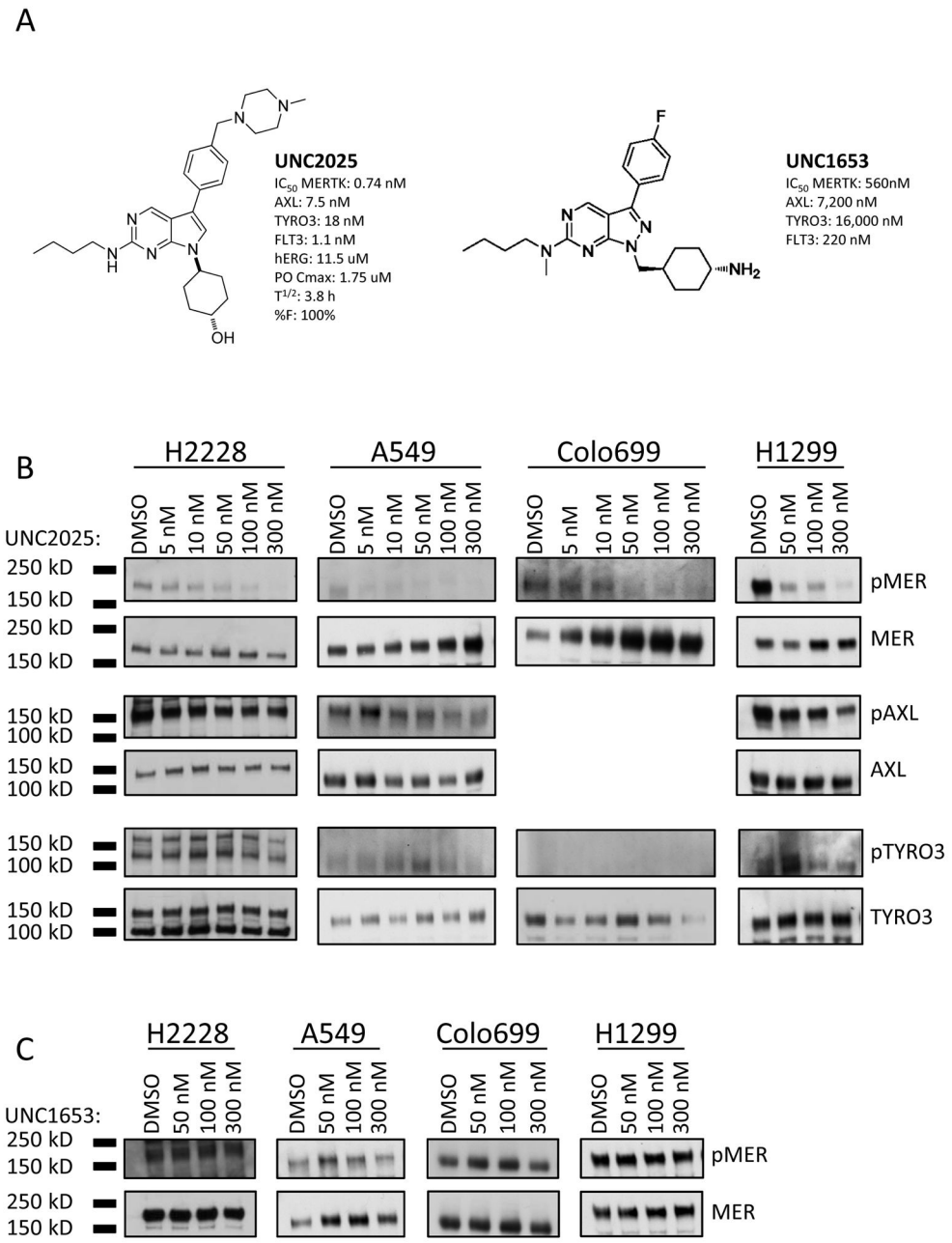

Figure 1.

UNC2025 Selectively Inhibits MERTK Activation. A) Structures of UNC2025 and UNC1653. B,C) H2228, A549, Colo699, and H1299 cells were treated with the indicated doses of UNC2025 (B) or negative control compound UNC1653 (C) for one hour prior to preparation of cell lysates. MERTK, AXL, or TYRO3 proteins were immunoprecipitated and phospho- and total proteins were detected by immunoblot.

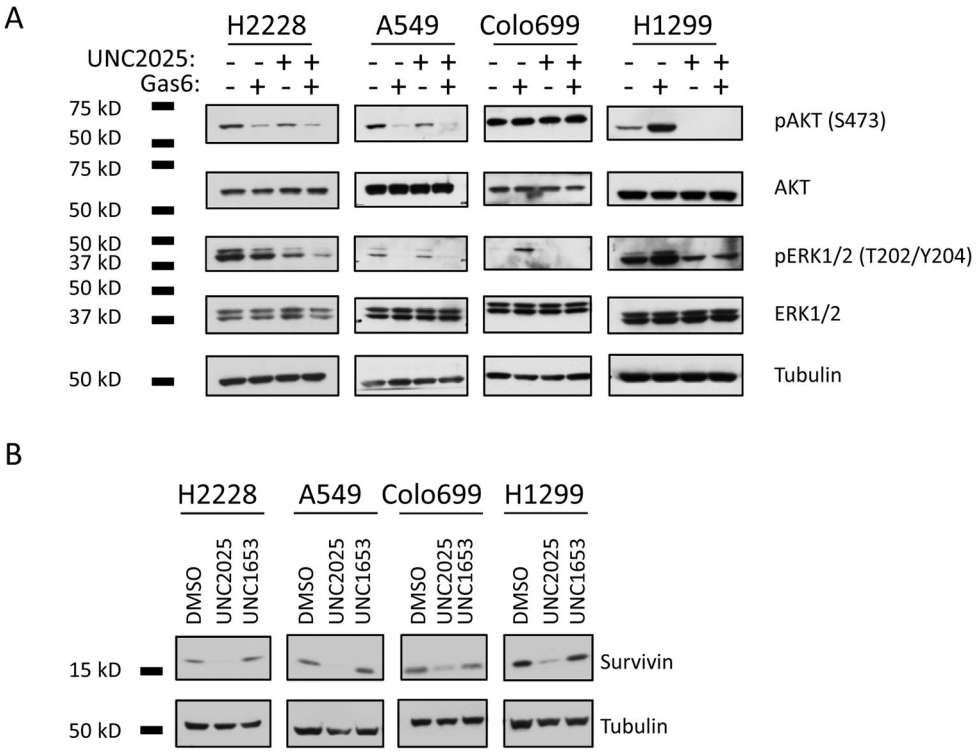

Figure 2.

UNC2025 Inhibits Signaling Pathways Downstream of MERTK. A) Sub-confluent cell cultures were starved for two hours in serum-free medium, and then treated with UNC2025 (300 nM) or an equivalent volume of DMSO vehicle for an additional two hours prior to stimulation with Gas6 (200 nM) for 10 minutes. Lysates were prepared and phospho- and total AKT and ERK1/2 were detected by immunoblot. B) Cells were treated with 300 nM UNC2025, UNC1653, or DMSO vehicle control for 72 hours in RPMI medium supplemented with 10% FBS, penicillin (100 U/mL), and streptomycin (100 μg/ml). Lysates were prepared and Survivin was detected by immunoblot.

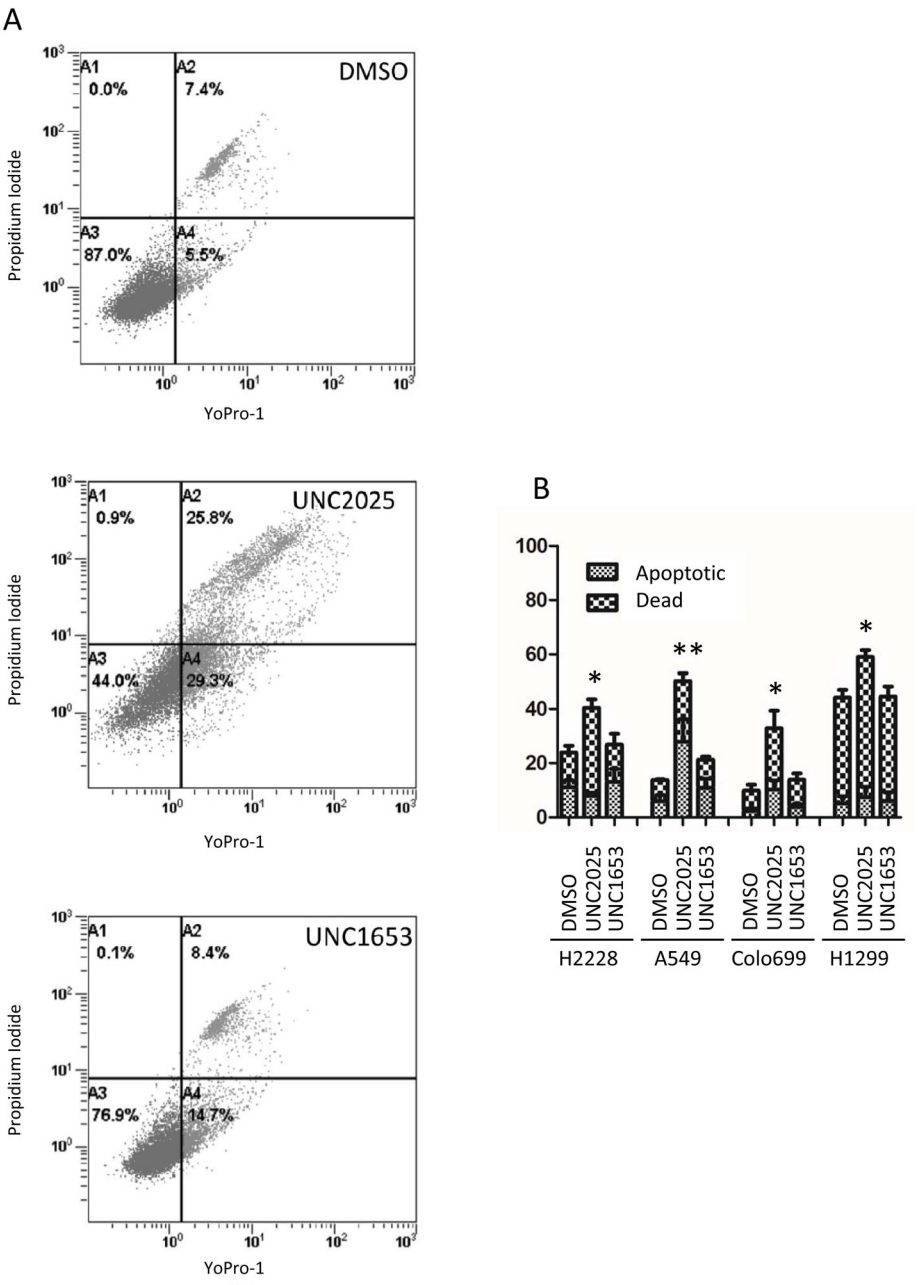

Figure 3.

UNC2025 Induces Apoptosis in NSCLC cells. H2228, A549, Colo699, and H1299 cells were treated with 300 nM UNC2025, UNC1653, or DMSO vehicle for 72 hours in RPMI medium supplemented with 10% FBS, penicillin (100 U/mL), and streptomycin (100 μg/ml), prior to staining with YO-PRO®-1 iodide (YO-PRO-1) and propidium iodide (PI) dyes and assessment of dye uptake by flow cytometry. Early apoptotic cells are stained selectively with YO-PRO-1, while late apoptotic and dead cells take up both dyes. A) Representative histograms for the H1299 cell line are shown. B) Mean values and standard errors derived from 3 independent experiments are shown (*P<0.05, **P<0.01).

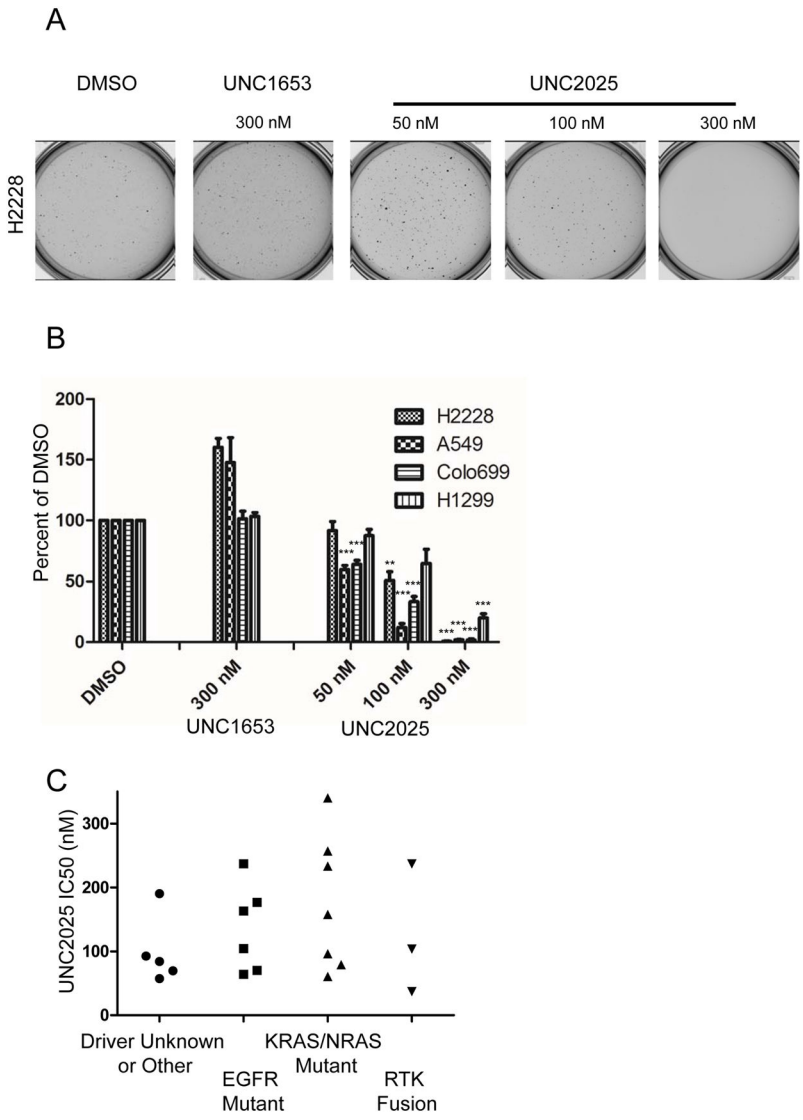

Figure 4.

UNC2025 Inhibits Colony Formation in Soft Agar. The indicated cell lines were cultured in 0.35% Noble Agar overlaying 0.5% Noble Agar in 6-well plates. Agar layers were overlaid with a medium layer containing UNC2025, UNC1653, or DMSO vehicle. The medium layer was aspirated and replaced three times a week for two weeks, after which time cells were stained with NTB and counted on a colony counter. A) Representative cultures of the H2228 cell line are shown. B) Mean colony numbers and standard errors derived from at least 3 independent experiments are shown (**P<0.01, ***P<0.001). C), IC_{50} values were calculated from soft agar data generated using a large panel of NSCLC cell lines with different genetic driver mutations. IC_{50} values (nM) are as follows: Driver Unknown or Other – Calu3: 90.7, Colo699: 69.6, H226: 57.3, H322: 190.4, H2126: 97.5. EGFR Mutant – H1650: 236.8, H1975: 70.0, H3255: 204.5, HCC827: 182.5, HCC4006: 88.8, HCC4011: 62.7. KRAS/NRAS Mutant – A549: 60.5, H157: 256.8, H358: 78.9, H441: 233.2, H460:

96.0, H1299: 157.6, H2009: 339.8. RTK Fusion – H2228: 91.6, H3122: 238.6, LC-2/ad: 37.4.

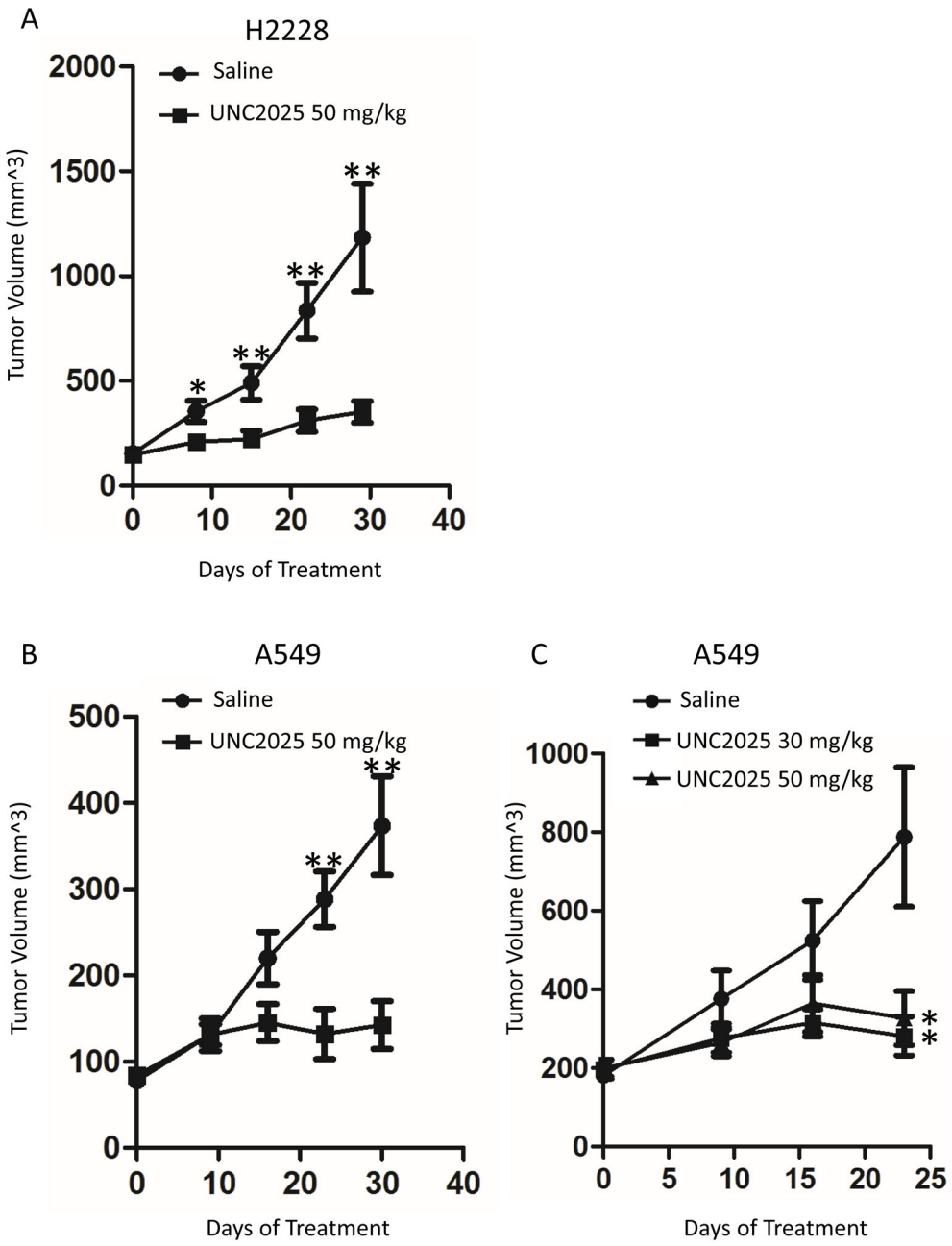

Figure 5.

UNC2025 Inhibits NSCLC tumor growth *in vivo*: H2228 (A) or A549 (B,**C**) cells were injected subcutaneously into the flanks of Nude mice and tumors were established until an approximate average volume of 150 mm^3 (A), 100 mm^3 (B), or 200 mm^3 (C). Mice were then treated twice daily by oral gavage with 50 mg/kg UNC2025, 30 mg/kg UNC2025 (C only), or 10 ml/kg saline vehicle. Tumors were measured weekly until study completion. In (A), data from two independent experiments were combined, for a total of 11 saline-treated mice and 12 UNC2025-treated mice; in (B) there were 9 saline-treated mice and 10

UNC2025-treated mice; and in (C) there were 6 saline-treated mice and 7 mice in each of the UNC2025 treatment groups. (*P<0.05, **P<0.01)